Section 1
ADVANCED TECHNOLOGY DEVELOPMENTS

1.A High-Efficiency Holographic Gratings for High-Power Laser Systems

Large-aperture holographic transmission gratings that possess high diffraction efficiency and high damage thresholds have been designed, fabricated, and experimentally tested within high-power, solid-state laser systems. The dispersive properties of diffraction gratings provide a variety of important and interesting techniques to control the spatial and temporal characteristics of laser light. Novel approaches to laser-beam smoothing and pulse shaping involve the transfer of information between time and space by means of the angular spectral dispersion (ASD) and lateral time delay imposed by a diffraction grating onto a propagating laser beam. The surface-relief transmission grating, composed of periodic and contiguous grooves, provides a source of ASD and possesses the intrinsically high damage threshold required for use in high-power laser systems. Transmission gratings have been employed in the driver line of the OMEGA laser system for several years without occurrence of laser-induced damage. Improved phase-conversion techniques, necessary to reach ultra-uniform levels of irradiation uniformity on the OMEGA Upgrade laser system, require the use of large-aperture transmission gratings. In addition, novel pulse-compression, pulse-expansion, and pulse-shaping schemes can now deploy highly dispersive gratings.

Theoretical Modeling

The holographic transmission grating, based on surface relief of a transparent material, diffracts an incident beam of light into various directions according to the same diffraction-grating equation as pertains to the holographic volume and reflection gratings or conventionally ruled gratings. The generalized grating equation is[1]

$$d[\sin(\theta) - \sin(i)] = m\lambda, \tag{1}$$

where d is the groove spacing, θ and i are the diffracted and incident angles, respectively, m is the diffraction order, and λ is the wavelength of light. Figure 50.1 shows an enlargement of a section of the surface relief. The periodic thickness variation constitutes a surface relief whose groove spacing and relief height (h) are typically of the order of the wavelength of light.
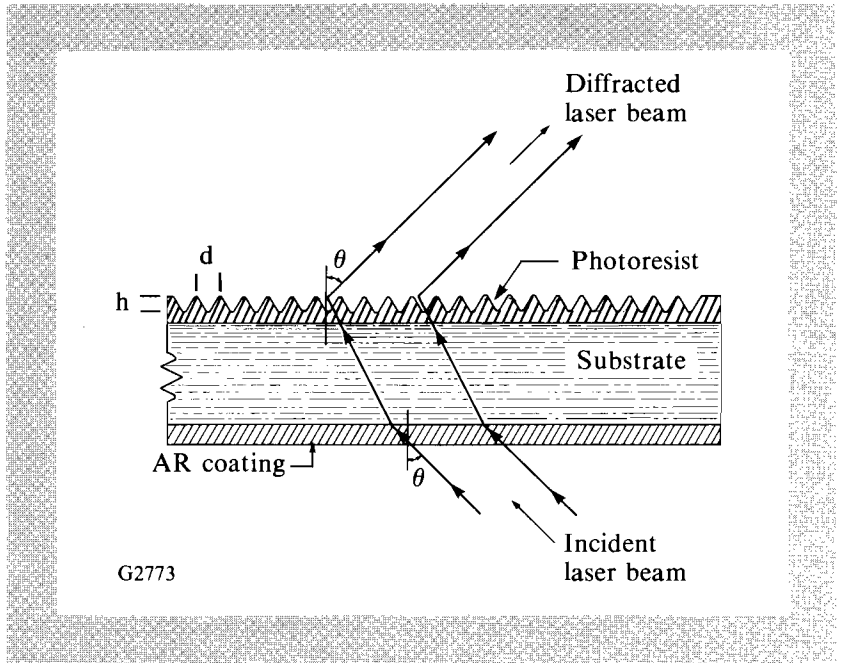

Fig. 50.1
A periodic thickness variation constitutes a surface relief that can diffract an incoming beam of light into an alternate direction. Holographic transmission gratings possess a groove spacing and surface-relief height typically of the order of the wavelength of light.

The rate of change of the diffraction angle with respect to change in wavelength is referred to as the angular dispersion (Γ) of the grating and is a measure of the angular spreading of the spectral components of light. Angular dispersion is given by

$$\Gamma = m / d \cdot \cos(\theta) . \tag{2}$$

For the special case of unit lateral magnification between the input beam and the output beam, where the incident and diffracted angles are equal but opposite, the expressions for the grating equation and angular dispersion become

$$2d \cdot \sin(\theta) = m\lambda \tag{3}$$

and

$$\Gamma = 2 \cdot \tan(\theta) / \lambda , \tag{4}$$

respectively. These equations describe the ray directions of spectral components, but do not contain information about the efficiency with which the diffraction occurs.

The diffraction characteristics of a dielectric grating have been the subject of much research. Numerical solutions have been obtained for gratings of arbitrary profiles by the integral-equation and differential-equation methods.[2,3] The differential-equation methods involve either a normal mode expansion or a coupled-wave expansion. Each represents a large system of equations and is difficult to handle computationally. The integral method[4] provides computational ease and has shown good agreement with experimental results for those gratings fabricated in the past. Theoretical predictions,[5] using an integral-equation code, show that peak diffraction efficiency near unity can be achieved over a wide range of groove spacings, or design angles, as shown in Fig. 50.2(a). For each design angle, the peak diffraction efficiency is obtained at a particular value for the groove aspect ratio h/d, which is determined by the temporally integrated energy reaching the photoresist. Figure 50.2(b) illustrates the dependence of diffraction efficiency on the aspect ratio of the grooves. This curve points out the importance of obtaining uniform and accurate exposures, since changes in groove aspect ratio cause changes in diffraction efficiency.
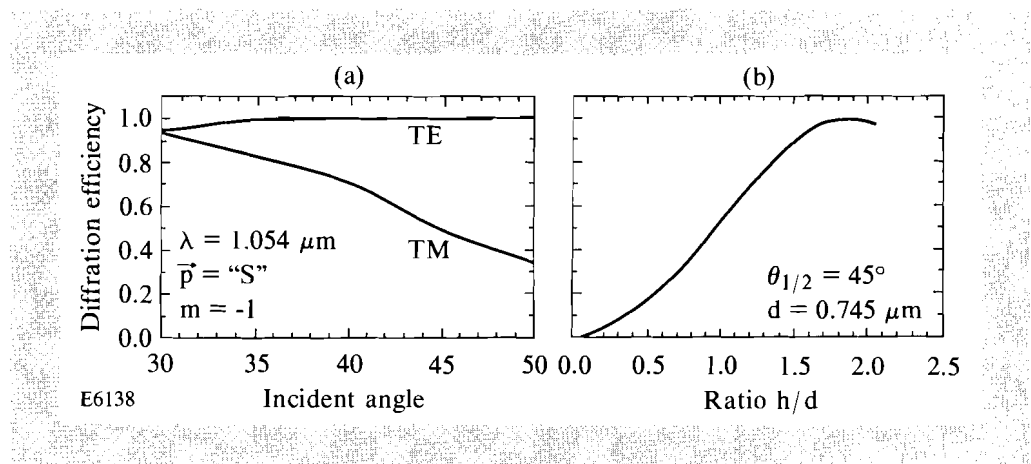

Fig. 50.2
Theoretical predictions [Fig. 50.2(a)] show that the peak diffraction efficiency approaches unity over a wide range of groove spacings or design angles. Diffraction efficiency varies with the aspect ratio of the grooves [Fig. 50.2(b)].

Interferometer Design

The holographic interferometer, as shown in Fig. 50.3, consists of a laser source, beam-conditioning optics, and two beamlines that intersect at the final recording plane. Several new and unique design features contribute to its overall capability for producing high-visibility interference fringes and a deep-grooved surface relief.

The laser is a Spectra-Physics 2045E argon ion laser, equipped with an intracavity etalon, highly dispersive cavity mirrors, and electronic feedback control to maintain both beam power and beam centering. At a 28-W output power in the visible, this laser is capable of 7-W output for simultaneous lasing of all of its ultraviolet lines. Selection of a single longitudinal mode within the $\lambda = 364$ nm spectral line, by using an intracavity etalon and a Fabry-Perot spectrum analyzer, further restricts the maximum output power to approximately 1 W. The laser is located on a separate table to prevent vibrations caused by the cooling system from reaching the interferometer. Vibrations of this type degrade fringe visibility and must be reduced as much as possible.
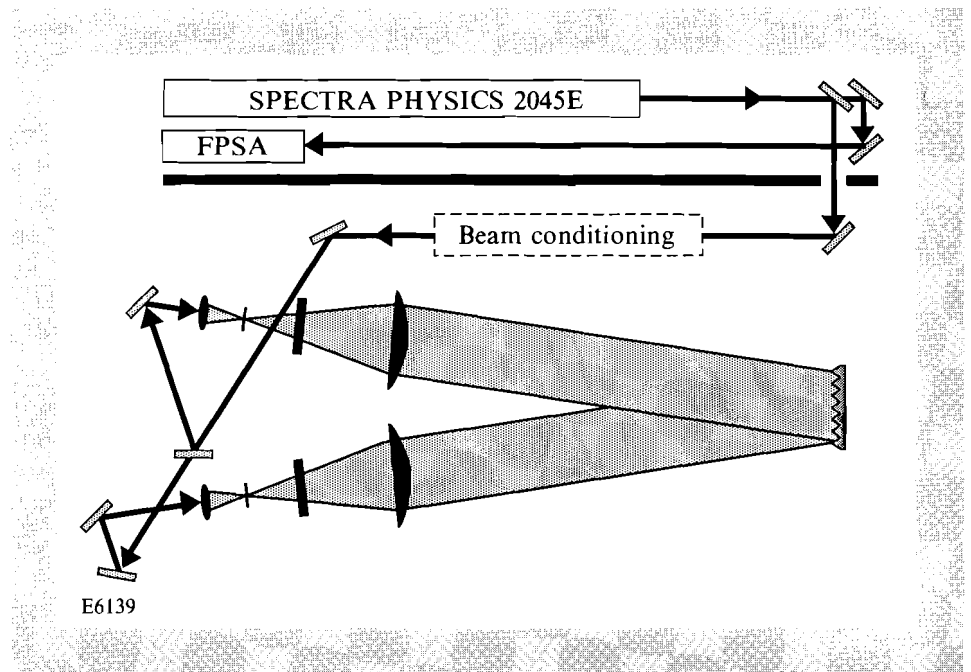
SPECTRA PHYSICS 2045E

FPSA

Beam conditioning

E6139

Fig. 50. 3

A beam scanner, a normal-incidence beam splitter, and an even mirror configuration are key design features of the new holographic interferometer. This system provides uniform exposure of the grating while maintaining stable interference fringes.

Before being split into two separate beam paths, the laser beam is raster scanned in two dimensions using the displacement introduced by rotation of a parallel plate.[6] The plate of glass is mounted within a dual-axis rotation mount. The scanner includes a computer-controlled stepper motor geared to have the necessary angular resolution while producing linear scan dimensions of up to 11–15 mm. After exiting the laser scanner, the beam is transported to a second table supporting the interferometer, is split into two equal intensity beams, and is directed toward two separate telescopes. The beam-splitter configuration is a critical factor in maintaining stable interference fringes at the recording plane, while simultaneously scanning the laser beam over the full aperture of the two arms of the interferometer.

The primary requirement to achieve a stable interferometer configuration involves splitting the light into two arms that gain equal amounts of increased path length when the beam is subjected to angular deviation prior to the split. This requirement is fulfilled both in sign and magnitude by using the following design criteria. First, the interferometer must maintain left-to-right sense between the two beamlines. This is achieved by setting the difference in the number of mirrors between the two beamlines to be an even number. Second, a compensating plate, with the same thickness as the beam splitter, must be placed within the transmitted beam at the same angle of incidence that exists for the beam splitter. The beam that reflects from the back surface of the beam splitter acquires the same optical path difference as the beam that transmits through both the beam splitter and the compensating plate.

This is the same criteria that was established for the Michelson interferometer,[7] which used an incoherent white light source. The principles of the Michelson interferometer are now being extended to coherent laser light to achieve stable interference fringes during two-dimensional scanning of the laser beam. This

design principle provides greatly reduced sensitivity to both laser mispointing during exposure, and angular rotation of the laser beam during scanning. In addition, parallel beam displacement is used as the beam-scanning technique, rather than angle scanning, to eliminate virtually all sensitivity to pre-splitter beam motion.

The two upcollimating telescopes, one within each arm of the interferometer, consist of an input objective, a spatial filter assembly, and an output collimating lens. Refractive telescopes are chosen to minimize sensitivity to vibration and reduce wavefront error. All optical elements—lenses, mirrors, beam splitters, and recording materials—are rigidly mounted to reduce vibration effects. In addition, the table for the interferometer is isolated from building vibrations by four pressurized support legs. To further isolate the system from vibration sources, thermal sources, and turbulence, it is located in a "room within a room" environment. In practice, it is found that the holographic system performs best during late night hours when most perturbation sources are reduced or absent.
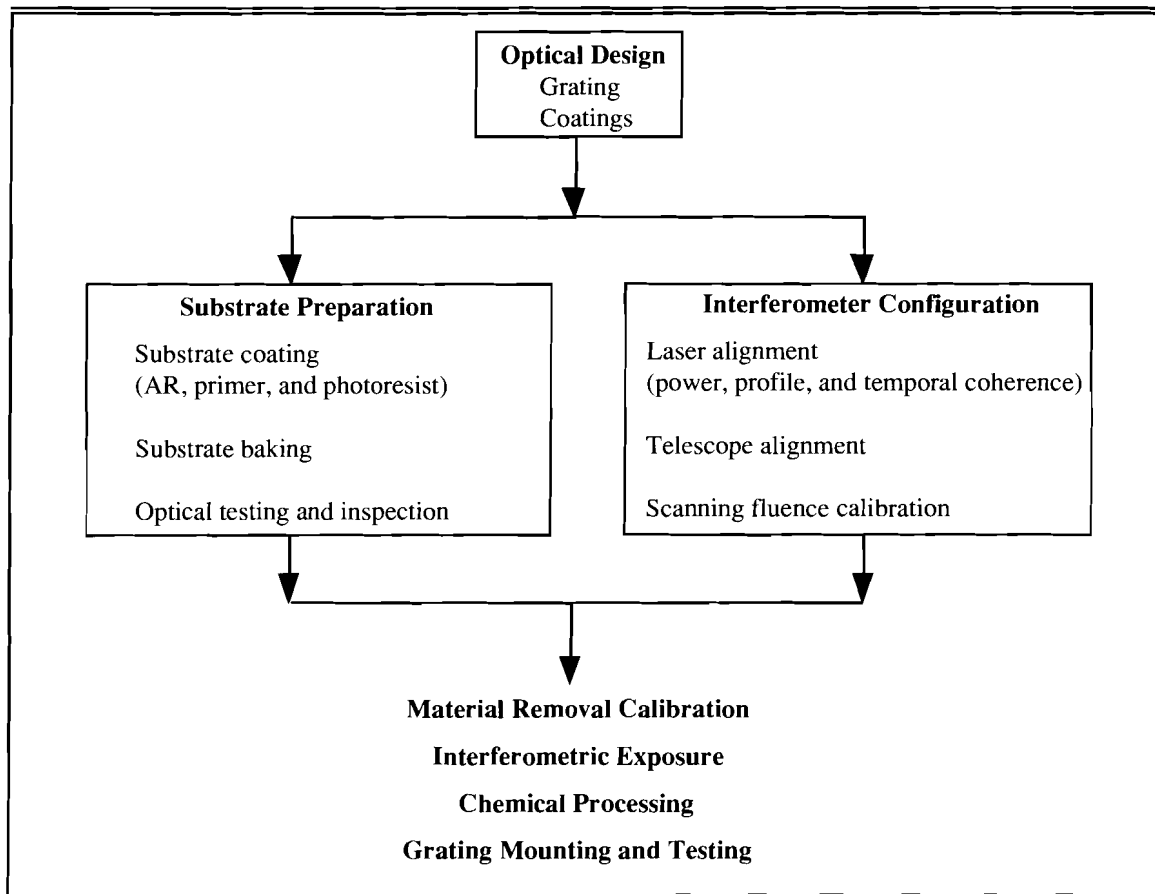
Grating Fabrication

The fabrication of holographic diffraction gratings involves a combination of photolithographic and interferometric processes involving a variety of optical and chemical techniques. Highlights of the fabrication process are outlined in the flowchart shown in Table 50.I. The design of a holographic grating involves the determination of proper groove profile (width, height, and shape) and the selection of optical materials used for the substrate (anti-reflection coatings and surface-relief layer). Two activities are performed after the grating is designed. Substrate preparation includes application of three thin-film coatings: an anti-reflection coating, a primer, and a photosensitive resist layer. This is followed by a baking of the substrate to remove the majority of the resist solvent. Optical inspection of the surfaces and high-resolution wavefront analysis of the optic complete the substrate preparation procedure.

In parallel with this activity, the interferometer is configured according to the grating size and groove width required. First, the laser source is aligned to operate at the necessary power output with a single longitudinal mode and single spatial mode. Second, the beam transport, scanner, and telescope optics are aligned. Third, laser scanning onto a photodetector is performed to determine the effective time-averaged fluence at the recording plane.

Once this calibration is complete, a non-interferometric exposure is applied to a resist-coated sample to quantify the relationship between exposure and material removal. These results determine both the bias exposure and the interferometric exposure needed to produce the required surface-relief profile. Exposed photoresist is developed in a sodium hydroxide and water mixture according to predetermined relationships between the baking time, the exposure, and the developer concentration. Once the grating has been chemically developed, grating mounting, efficiency measurements, and wavefront testing are performed as the final steps of the procedure.

Table 50.I: The fabrication of holographic diffraction gratings involves a combination of photolithographic and interferometric processes utilizing a variety of optical and chemical techniques.

Optical Design
Grating
Coatings

Substrate Preparation

Substrate coating
(AR, primer, and photoresist)

Substrate baking

Optical testing and inspection

Interferometer Configuration

Laser alignment
(power, profile, and temporal coherence)

Telescope alignment

Scanning fluence calibration

Material Removal Calibration

Interferometric Exposure

Chemical Processing

Grating Mounting and Testing

E6238

The scanning electron microscope (SEM) is used to characterize the surface relief of the holographic grating that exhibits unity diffraction efficiency. The size and shape of the grooves are shown in Fig. 50.4. Close-up examination of the grooves shows that the profile is nonsinusoidal. A measured diffraction-efficiency verses incident-angle curve, shown in Fig. 50.5, indicates greater angular sensitivity than that predicted for the optimum sinusoidal groove shape. In addition, it has been found that grating efficiency is less sensitive to mean exposure than is theoretically predicted. This relative insensitivity to mean exposure, the observed increase in angular sensitivity, and the SEM determination of nonsinusoidal groove shape can potentially be explained by ultrahigh visibility together with a material-removal saturation effect. Although this effect needs to be characterized further for applications in grating replication, gratings of unity efficiency have immediate applications prior to obtaining a complete understanding.
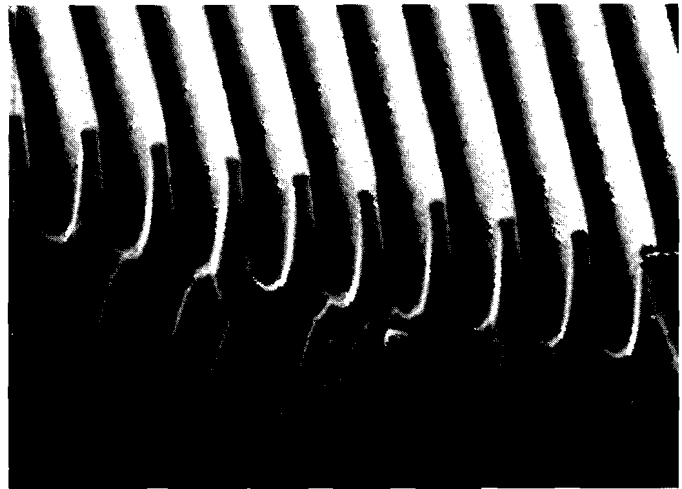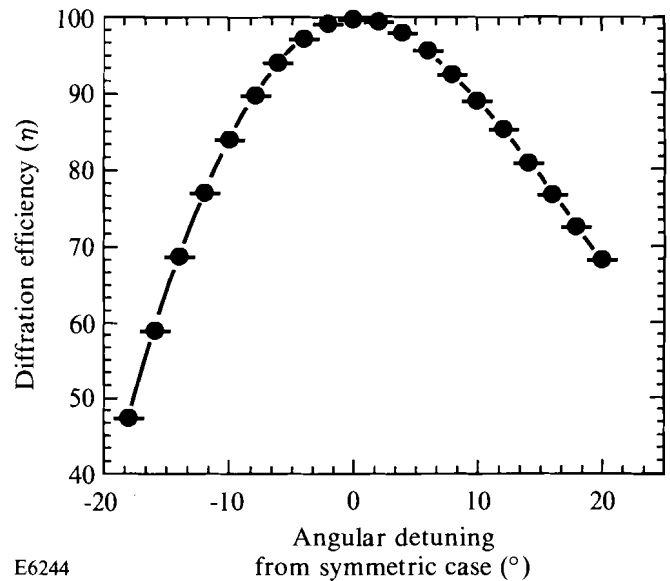
Fig. 50.4
Close-up examination of a holographic diffraction grating, using the scanning electron microscope (SEM), shows that the surface relief of a high-efficiency grating is nonsinusoidal.

E6140

Fig. 50.5
100% intrinsic diffraction efficiency has been demonstrated with nonsinusoidal surface relief. Theoretical modeling predicts the diffraction efficiency of a holographic grating to possess a weak dependence on the incident angle as shown by the gradual variation in the solid curve. Experimental measurements of the actual surface-relief profile show a greater angular sensitivity.

E6244

Laser Applications

A wide variety of applications exist for high-efficiency, high-damage-threshold, holographic diffraction gratings. Currently, a set of gratings designed for infrared ($\lambda = 1054$ nm) laser light is used in the driver line of the OMEGA system to provide the angular dispersion required for laser-beam smoothing.[8] Several sets of holographic gratings, with a greater amount of angular dispersion, will be required for the driver lines of the OMEGA Upgrade laser. In addition, as schematically illustrated in Fig. 50.6, broadband frequency conversion can be accomplished with gratings placed on either side of the frequency-conversion crystals. Spectrally resolved phase matching within the tripler is achieved with
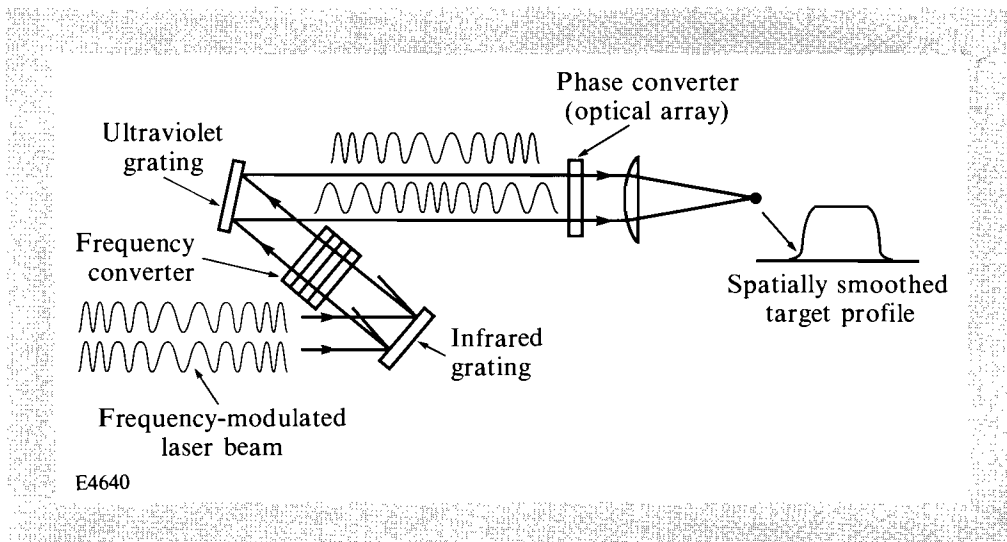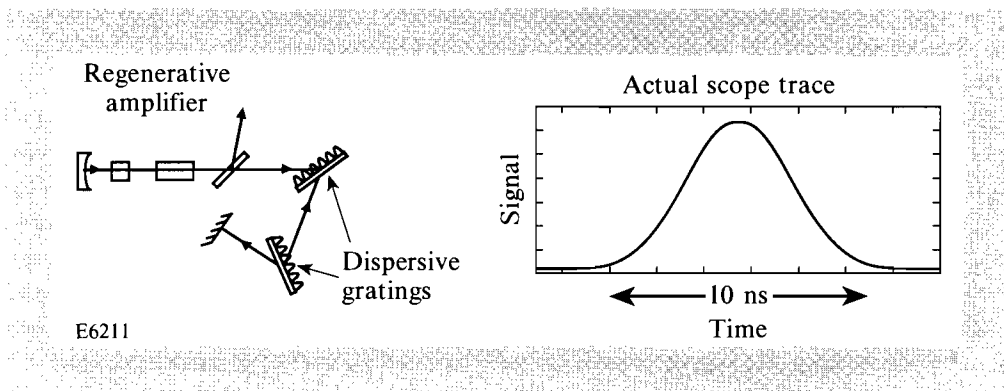
Fig. 50.6
Broadband frequency tripling and phase conversion can be achieved with infrared and ultraviolet diffraction gratings. They are placed on either side of the KDP crystals used for frequency conversion of the high-power, infrared laser light.

the infrared grating, while the desired amount of color cycling is obtained by partially cancelling the angular dispersion caused by the infrared grating with the angular dispersion of an ultraviolet grating.

Other applications for infrared gratings include pulse expansion, pulse compression, and pulse shaping of pulsed laser beams. In each of these schemes, highly dispersive transmission gratings provide several design advantages. They offer greater dynamic range, compactness, high damage threshold, and high diffraction efficiency. As shown in Fig. 50.7, highly dispersive gratings, placed within a regenerative amplifier, can be used to increase spectral purity of the light inside the laser cavity. The pulse width of a Fourier-transform-limited laser pulse is increased as its bandwidth is decreased. To demonstrate this use of holographic gratings, a 50-ps pulse has been stretched to over 5 ns by using a grating with 200 μrad per angstrom angular dispersion. Pulse expansion to 10 ns is possible using the configuration in Fig. 50.7. As another example of the pulse-width control offered by transmission gratings, Fig. 50.8 shows a scheme for pulse compression accomplished using four high-damage-threshold holographic gratings. A rigidly mounted thin substrate is used for the fourth grating to minimize nonlinear beam effects. Alternate strategies of reducing the amount of nonlinear phase are being investigated.

Fig. 50.7
Highly dispersive transmission gratings, placed within a regenerative amplifier, are used to increase the spectral purity of the light inside the laser cavity. A 50-ps pulse is stretched to over 5 ns as a first demonstration of this use of holographic gratings.
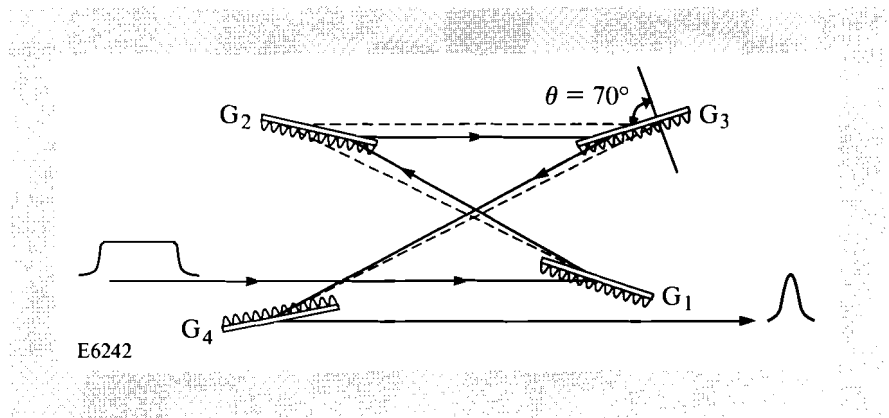
$\theta = 70°$

G₂ G₃ G₁ G₄ E6242

Fig. 50.8

Compression of a laser pulse with a duration of hundreds of picoseconds to a much shorter duration of a few picoseconds can be accomplished with four high-damage-threshold holographic gratings.

A novel method of pulse shaping (see Fig. 50.9), involving a mapping from time to space, followed by a spatial-filtering operation, and then a reverse mapping from space to time, is made more practicable using transmission gratings. An appropriately designed spatial filter located at the focal plane of the grating spectrometer gives rise to a pulse shape at the output of the second grating pair that is similar to the transmittance function of the filter. This pulse-shaping scheme is currently under development for use on the OMEGA Upgrade laser system.

Additional applications of high-power, high-dispersion transmission gratings involve its function as a spectral filter. These gratings provide excellent blocking capability at the Fourier plane for measurement of small-signal gain, for ASE suppression in amplifier subsystems, and many other situations, many of which remain to be demonstrated. Furthermore, the transmission grating, based on diffraction from a surface relief, provides several advantages for the design of spectroscopic instruments. Compact optical configurations capable of high angular dispersion and efficient over a broad wavelength range are possible. A highly dispersive and low-noise spectrometer is illustrated in Fig. 50.10.

Conclusion

High-efficiency holographic gratings, exhibiting unity diffraction efficiency, have been demonstrated for use in high-power laser systems. A novel interferometric technique, which incorporates parallel beam scanning and a pointing-insensitive optical configuration, is used to obtain uniform irradiation of the recording medium while maintaining stable interference fringes. Large-aperture gratings, covering a wide range of groove spacings, can be manufactured with this interferometric exposure technique. Numerous applications exist for these high-efficiency and high-damage-threshold holographic gratings. Laser-beam smoothing and pulse-shaping techniques, many of which have been invented and developed at LLE, incorporate these gratings at physical apertures ranging between several centimeters to tens of centimeters. In addition, highly dispersive holographic diffraction gratings are a central component to pulse-expansion and pulse-compression schemes.

Furthermore, these new gratings offer the possibility of building high-resolution and high-signal-to-noise spectroscopic instruments. Future research
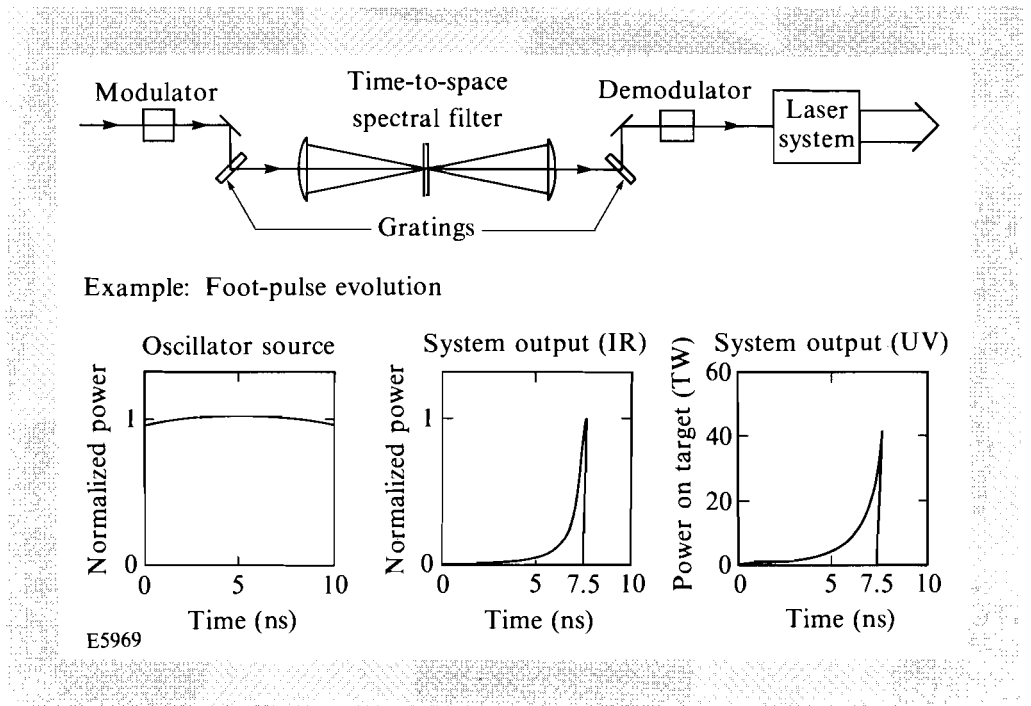
69

E5969

Fig. 50.9
Spectral pulse shaping involves a mapping from time to space, followed by a spatial-filtering operation, and then a reverse mapping from space to time. Placement of an apodizer at the focal plane of the grating spectrometer gives rise to a pulse shape, at the output of the second grating pair, similar to the transmittance function of the filter.

E6243

Fig. 50.10
The transmission grating provides several advantages for the design of spectroscopic instruments. Compact configurations capable of high angular dispersion and efficient over a broad wavelength range are possible.
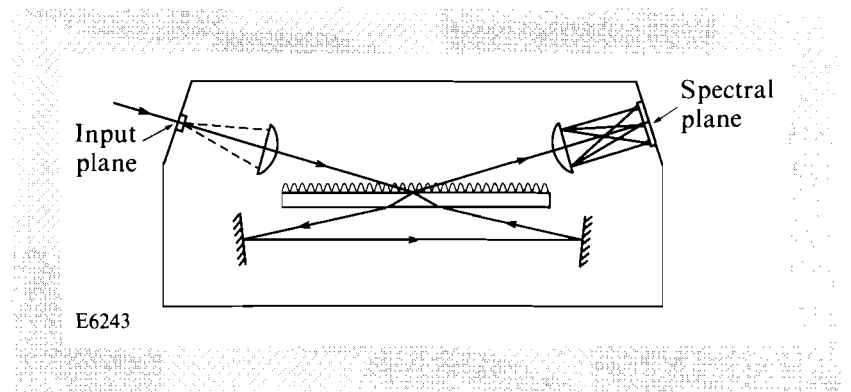
is aimed at the development of replication techniques necessary for the production of large-aperture ultraviolet gratings that would be used for broadband frequency conversion and phase conversion of laser light on the OMEGA Upgrade laser system.